Published in final edited form as:
J Neurochem. 2009 May ; 109(4): 1179–1191. doi:10.1111/j.1471-4159.2009.06055.x.

Bioenergetic Analysis of Isolated Cerebrocortical Nerve Terminals on a Microgram Scale: Spare Respiratory Capacity and Stochastic Mitochondrial Failure

Sung W. Choi, **Akos A. Gerencser**, and **David G. Nicholls**
Buck Institute for Age Research, Novato, CA 94945, USA

Abstract

Presynaptic nerve terminals (synaptosomes) require ATP for neurotransmitter exocytosis and recovery and for ionic homeostasis, and are consequently abundantly furnished with mitochondria. Presynaptic mitochondrial dysfunction is implicated in a variety of neurodegenerative disorders, although there is no precise definition of the term 'dysfunction'. In this study we test the hypothesis that partial restriction of electron transport through Complexes I and II in synaptosomes to mimic possible defects associated with Parkinson's and Huntington's diseases respectively, sensitizes individual terminals to mitochondrial depolarization under conditions of enhanced proton current utilization, even though these stresses are within the respiratory capacity of the synaptosomes when averaged over the entire population. We combine two novel techniques, firstly using a modification of a novel plate-based respiration and glycolysis assay that requires only microgram quantities of synaptosomal protein, and secondly developing an improved method for fluorescent imaging and statistical analysis of single synaptosomes. Conditions are defined for optimal substrate supply to the *in situ* mitochondria within mouse cerebrocortical synaptosomes, and the energetic demands of ion cycling and action potential firing at the plasma membrane are additionally determined.

Keywords

synaptosomes; mitochondria; membrane potential; respiration; imaging

While mitochondrial dysfunction is implicated in a wide range of neurodegenerative disorders, investigations employing isolated brain mitochondria have a number of limitations. Firstly the preparations are inherently heterogeneous, since 'non-synaptic' mitochondria originate from the cell bodies of both neurons and glia. Secondly, as with all isolated mitochondrial incubations, the environment and substrate availability depart considerably from the physiological. In contrast, isolated nerve terminals (synaptosomes) largely preserve the metabolism, mitochondrial function, plasma membrane excitability, receptors, ion channels and machinery for the exocytosis and reuptake of neurotransmitters characteristic of the intact presynaptic terminal *in situ* (for reviews see Nicholls, 1993, 2003; Sánchez-Prieto et al., 1996) and possess the considerable advantage in contrast to primary neuronal cultures that preparations can be made from experimental animals of any age, thus allowing critical age-related changes to be monitored.

While many studies of *in situ* mitochondrial function have been performed with synaptosomes by this and other groups, the amount of material required for monitoring

Address correspondence to: David G. Nicholls Buck Institute for Age Research, 8001 Redwood Boulevard Novato, CA 94945, USA Phone: (415) 209 2096 Fax: 9415) 209 2232 e-mail: dnicholls@buckinstitute.org.

respiration (typically 0.5mg synaptosomal protein) has severely restricted the application of this technique for studies of discrete brain regions of transgenic mice. In this study we report the application of the Seahorse XF24 extra-cellular flux analyzer (Wu *et al.* 2007) to monitor synaptosomal respiration together with extra-cellular pH as an indication of anaerobic glycolysis. The fifty-fold decrease in the amount of material required compared to conventional respirometry, together with the ability to assay multiple samples in parallel facilitates the study of synaptosomes from specific murine brain regions. In this study we first quantify basic mitochondrial respiratory parameters, including coupling efficiency and 'spare respiratory capacity' in the presence of optimal protonophore concentrations, establishing conditions for optimal substrate supply and then determining the bioenergetic demand of ion cycling at the plasma membrane.

Recent studies with primary neuronal cultures have emphasized the importance of spare respiratory capacity for maintaining an energetic reserve in the face of oxidative stress (Vesce *et al.* 2005), partial Complex I inhibition (Yadava and Nicholls 2007) or in a model of 'mild-uncoupling' (Johnson-Cadwell *et al.* 2007). In this study we extend this to synaptosomes by *in vitro* restriction of Complex I and II activity to decrease spare respiratory capacity modeling putative aspects of Parkinson's and Huntington's diseases. By developing an improved technique for the functional imaging of single discrete synaptosomes it is possible to monitor stochastic changes in mitochondrial membrane potential ($\Delta\psi_m$) between individual synaptosomes in these respiratory-restricted models. A heterogeneous response to increased energy demand, together with a time-dependent decrease in $\Delta\psi_m$ indicates that sub-populations of synaptosomes are differentially susceptible to bioenergetic failure under these conditions. The suitability of these exquisitely sensitive techniques for examining subtle bioenergetic changes in discrete brain regions of transgenic mouse models of neurodegenerative disorders is discussed. .

Materials and Methods

Reagents

Tetramethylrhodamine methyl ester, TMRM, was from Invitrogen (Carlsbad, CA). All other reagents were from Sigma-Aldrich (St. Louis, MO).

Preparation of synaptosomes

Synaptosomes were isolated from CD1 mouse cerebral cortices aged from 17-21days by the method of Dunkley et al. (1986) with slight modifications. Briefly, a cortex (0.1-0.2g/brain) was rapidly removed, rinsed with ice-cold 'Sucrose Medium' (320 mM sucrose, 1 mM EDTA, 0.25 mM dithiothreitol, pH 7.4) to remove excess blood, transferred to a pre-chilled Dounce glass homogenizer containing 3 ml Sucrose Medium and homogenized gently by 8-10 up-and-down strokes. The homogenate was then centrifuged at 1000g for 10 min at 4°C. The supernatant was carefully layered on top of a discontinuous Percoll gradient (3ml layers of 3, 10 and 23% Percoll in Sucrose Medium) in a 15ml centrifuge tube, and centrifuged at 32500g for 10 min at 4°C in a JA-25.50 fixed angle rotor in a Beckman Avanti J-26 XPI centrifuge. Synaptosomes were isolated as the band between 10% and 23% Percoll. It should be noted that resealed glial membranes (gliosomes) have been isolated from a 2-6% Percoll boundary (Stigliani *et al.* 2006).

The synaptosomal band was diluted into 'Ionic Medium' (20 mM HEPES, 10 mM D-Glucose, 1.2 mM Na_2HPO_4, 1 mM $MgCl_2$, 5 mM $NaHCO_3$, 5 mM KCl, 140 mM NaCl, pH. 7.4) or diluted into 'Sucrose Medium'. Both were centrifuged at 15000g for 15 min at 4°C to remove Percoll. The final synaptosome pellets were resuspended in Ionic or Sucrose media respectively in prior to respirometry or confocal imaging.

Synaptosomal attachment

Seahorse respirometry and confocal imaging each require that synaptosomes be robustly attached to the substrate. The polystyrene Seahorse plates and glass-bottomed 96 well plates were each coated with polyethyleneimine (1:15000 dilution from a 50% solution, Sigma-Aldrich, St. Louis) to optimize attachment. While there are a number of studies in which synaptosomes in ionic media have been allowed to sediment under unit gravity onto coverslips coated with Cell-Tak (BD Biosciences, San Jose, CA) (Nichols and Mollard, 1996; Nayak et al., 2001) or poly-D-lysine (Millán et al., 2002), the relatively high frequency of aggregates rather than discrete single synaptosomes has limited the ability to image multiple discrete terminals in a single field.

Synaptosomes aggregate when suspended in a medium with a significant ionic strength but remain discrete in a sucrose-based isolation medium with very low ionic strength. Respirometry and confocal imaging have rather different requirements, thus for the former it is important to optimize the yield of attached synaptosomes and to ensure that attachment is sufficiently firm to preclude displacement of the terminals during the rather vigorous mixing that occurs prior to each determination in the XF24 respirometer (Fig. 1b). For confocal imaging, in contrast, yield is of secondary importance, but it is preferable to optimize an even field of attached ‘monmeric’ synaptosomes where individual terminals can be distinguished. Preliminary experiments determined that an ionic medium gave a high yield optimal for respirometry, while the sucrose-based preparation medium yielded a uniform field of monomeric synaptosomes for imaging (Fig. 1c). The diameters of the images equilibrated with TMRM (Fig. 1d) were consistent with single discrete synaptosomes (Jones and Brearley, 1973).

Respiration and medium acidification rates

For monitoring respiration, ‘Ionic’ synaptosomes (10μg protein/well unless otherwise shown) were aliquoted into 20 wells of a polyethyleneimine-coated XF24 V7 cell culture microplate (Seahorse Bioscience, North Billerica, MA). The plate was centrifuged at 3400g for 1hr at 4°C in an A-4-62 rotor in a Eppendorf 5810R centrifuge. Control experiments determined that this caused an attachment of synaptosomal aggregates that was sufficiently robust to withstand the mixing protocols of the machine. The Ionic medium was replaced with 700μl of ‘Incubation Medium’ (3.5mM KCl, 120mM NaCl, 1.3mM $CaCl_2$, 0.4mM KH_2PO_4, 1.2mM Na_2SO_4, 2mM $MgSO_4$, 15mM D-glucose, 4mg/ml BSA, 37°C). Plates were used immediately or stored on ice for not more than 3hrs. The cell culture microplate was incubated and loaded into the Seahorse XF24 extracellular flux analyzer following the manufacturer's instructions. All experiments were performed at 37°C. The XF24 utilizes a specialized multi-well plate, lowering an array of sensors to enclose a 7μl fluid volume above a layer of attached cells (or in this case synaptosomes) in 24 wells each with a total volume of approximately 700μl. During the 1-3min period when the volume is enclosed oxygen uptake and medium acidification are monitored by fluorescence probes immobilized in matrices attached to the sensor, which is subsequently raised and oscillated to ensure mixing and reoxygenation with the bulk medium prior to the next measurement or addition of reagents as appropriate. Oxygen consumption and acidification rate data points reefer to the mean rates during the measurement cycles, which consisted of a mixing time of 30s and a wait time of 2min followed by a data acquisition period of 3min (13 data points). All reagents were added at appropriate dilutions in 75μl of Incubation Medium.

The oxygen concentration in the 7μl entrapped volume was sensed by the O_2-quenched fluorescence of the probe. The non-linear response of the probe was calibrated with the Stern-Volmer equation. The oxygen consumption rates were determined by using a compartment model based ‘deconvolution’ algorithm which compensated for oxygen

diffusion phenomena occurring around the entrapped volume, and for the response time of the probe (Gerencser et al. unpublished results). Rates obtained with this algorithm were proportional to the amounts of synaptosomes attached to the plate, and were steady during basal respiration (not shown). Most respiration rates are expressed as a percentage of the basal respiration in Incubation Medium (containing 15mM glucose) except where absolute rates are reported. The rate of acidification of the medium was monitored in parallel. Results were normalized relative to the basal acidification rate of synaptosomes in glucose medium.

Confocal microscopy

For single synaptosome confocal imaging 'Sucrose' synaptosomes (3μg protein/well) were aliquoted into a 4×3 subset of wells in a Whatman 96-well glass-bottomed multi-well plate and centrifuged in parallel with the 'Ionic' synaptosomes. Synaptosomes were subsequently loaded with 10nM tetramethylrhodamine methyl ester (TMRM) plus 1μM tetraphenylboron for 40min. Fluorescence was monitored in a Zeiss LSM510 confocal microscope with a Plan-Apochromat 40×/0.95 air objective, at 543nm excitation and >560nm emission using the 'Multi Time Lapse' module of the Zeiss LSM software. Single planes of 512×512 images at 0.088 μm/pixel resolution were recorded at ~9 min intervals, and each image acquisition was preceded by auto focusing.

Analysis of mitochondrial membrane potentials in single synaptosomes

Time lapse image sequences were aligned to stabilize any lack of register in sequential images due to inaccuracy of the x,y-stage motors. This was done based on the transmitted light images recorded in parallel with the TMRM signal. The background was subtracted at the first percentile of the image histograms. Then a duplicate of the TMRM fluorescence image series was band pass spatial filtered at ω=0.55-2 μm/cycle (Gerencser and Nicholls 2008) to enhance details corresponding to synaptosome-sized objects and reduce noise. This was followed by binarization at Otsu's optimum threshold value (Otsu, 1979). Individual synaptosomes (sized at least 10 pixels in area and maximally 20 pixels in diameter) were located by segmentation of binarized images, and their positions were tracked throughout the time sequence. Fluorescence intensities corresponding to each segment were determined in the original, background subtracted, TMRM fluorescence images, yielding a time lapse of fluorescence intensities for each individual synaptosome. For synaptosomes that gained or lost TMRM fluorescence signal during the experiment, intensities were measured at the first or last known position. Finally the TMRM signal (F) was normalized to the mean of the two baseline data points (F_0) and converted to millivolts relative to the baseline by calculating $26.7\ \text{mV} \times \ln((F- F_0)/F_0+1)$. Therefore the negative sign denotes depolarization.

To visualize populations, histograms of changes in $\Delta\psi_m$ of single synaptosomes were calculated in Mathematica 5.2 (Wolfram Research, Champaign, IL). At t=0 the relative $\Delta\psi_m$ of each synaptosome in a field wasdefined to be zero (and was therefore omitted from the histogram). At approximately 9min intervals images of the field were taken and the *change* in potential from t=0 recorded. A range of +20mV (hyperpolarization0 to −50mV (depolarization) was divided into 40 bins and the percentage of synaptosomes in each bin was plotted. Image processing was carried out using custom developed image analysis software written in Pascal language (Delphi 2009; Borland, Austin, TX) and Mathematica 5.2.

Statistical analysis

Respiration and acidification rates are presented as the mean ±s.e.m. of at least three independent experiments with different synaptosomal preparations. Membrane potential data is shown as the mean±s.e.m. of the parameters calculated from independent synaptosomal preparations (n). Histograms reflect data pooled from all experiments performed.

Significance level was determined by performing ANOVA on the complete data set with Tukey's *post-hoc* testing.

Results

Coupling efficiency and spare respiratory capacity

Isolated nerve terminals utilize exogenous glucose and pyruvate as substrates (Kauppinen and Nicholls, 1986b). Fig. 2 and Table 1 show mean results from multiple experiments for synaptosomes respiring in the presence of 15mM glucose, 10mM pyruvate as sole substrate and 15mM glucose supplemented with 10mM pyruvate. Coupling efficiency under these conditions is estimated by the addition of oligomycin, and spare respiratory capacity by the addition of FCCP. It should be emphasized that in all experiments the concentration of FCCP was titrated to just relieve respiratory control. Under these conditions there is predicted to be only a slight decline in $\Delta\psi$ (Johnson-Cadwell et al., 2007).

In order to assess the extent to which electron transport chain activity controls spare respiratory capacity it is important to consider whether substrate supply to the *in situ* mitochondria is optimal. Using conventional oxygen electrode assemblies, we have previously determined that pyruvate is an excellent substrate for intact synaptosomes and can further enhance the respiration in the presence of 15mM glucose (Kauppinen and Nicholls, 1986b). Fig. 2b and c show the respiratory parameters for synaptosomes respiring in the presence of 10mM pyruvate and with both pyruvate and 15mM glucose present. It is apparent that exogenous pyruvate and glucose are almost additive in enhancing spare respiratory capacity in the presence of FCCP. In addition to enhancing the basal respiration in the presence or absence of glucose it is notable that pyruvate significantly increases the proton leak conductance estimated from the oligomycin-insensitive respiration (Table 1).

Since proton leak rate is highly dependent upon $\Delta\psi_m$ (Nicholls 1974) and pyruvate produces a mean population hyperpolarization of the intra-synaptosomal mitochondria by about 6mV even in the presence of glucose (Kauppinen and Nicholls 1986b), one explanation is that the increased proton leak may be accounted for by this increased driving force. However, an alternative hypothesis is that pyruvate selectively energizes a population of synaptosomes that has impaired glucose utilization and thus possess depolarized mitochondria. In order to monitor $\Delta\psi_m$ in individual synaptosomes, fields of 'monomeric' synaptosomes (see Methods) were equilibrated with $TMRM^+$ under non-quench conditions (Ward et al., 2000) and changes in $\Delta\psi_m$ were monitored with confocal microscopy (Fig. 3). It should be noted that strictly the fluorescence is a function of both $\Delta\psi_m$ and plasma membrane potential (Ward et al., 2000).

Single synaptosomes were tracked and the $TMRM^+$ fluorescence intensity was monitored as a function of time (Fig. 3). The deviation of $TMRM^+$ fluorescence intensity from the baseline of each individual synaptosome was expressed as mV change. Therefore at 0 min 100% of synaptosomes were at '0 mV' in the histograms. At later time points the population of synaptosomes was represented by the bell-shaped distributions of membrane potential change. The superimposed color-coded histograms show a time-dependent widening of the distribution (increase in the variance), emphasizing the stochastic deviation of $\Delta\psi_m$ from the value at 0 min in individual terminals.

When synaptosomes utilized glucose alone (Fig. 3A) the mean $\Delta\psi_m$ slowly decayed, by 5±1.2 mV in 38 min (Fig.3A). In contrast, this decay was insignificant (0.45±0.49 mV) in glucose medium supplemented with 10mM pyruvate (Fig.3B). When pyruvate was added to synaptosomes kept in glucose medium, mitochondria hyperpolarized by 3.8±1.3 mV by 38 min (Fig.3C) and respiration increased by 22.9±0.6% (n=4) in a parallel respirometer

experiment, data not shown. The changes in potential were significantly different from each other at $p<0.05$ by one way ANOVA and pairwise comparison by Tukey *post-hoc* test. At 38min after pyruvate addition 2.6% of synaptosomes had hyperpolarized $\Delta\psi_m$ by more than 20mV, in contrast to only 0.3% of the synaptosomes in glucose medium and 0.5% in glucose plus pyruvate medium over the same period.

As shown by the images taken before (Fig. 3D) and after (Fig. 3E) pyruvate very few 'new' synaptosomes appeared in the $TMRM^+$ image, but rather there was a brightening in general. Thus the effect of pyruvate at a single synaptosome level is to cause a significant hyperpolarization. This, combined with the slow decline in $\Delta\psi_m$ in glucose alone suggest that glycolysis is not fully stable in synaptosomes incubated at 37°C, perhaps due to a slow leakage of glycolytic intermediates. Incubating synaptosomes in glucose-only medium, or addition of pyruvate, significantly widened the histogram of the $\Delta\psi_m$, increasing the standard deviation to 12.5±1.0 mV and 10.6±0.7 mV, respectively (both at $p<0.01$ significance at 38min), as compared to synaptosomes maintained throughout in glucose plus pyruvate medium (6.7±0.4 mV). This suggests that a population of synaptosomes showed a stochastic failure of glycolysis, and that this population could be rescued by the addition of pyruvate, the glycolytically less competent terminals producing stronger responses to pyruvate. For these reasons we have included 10mM pyruvate in the incubation to eliminate this factor in most of the subsequent experiments.

The contribution of anaerobic glycolysis

Synaptosomes display a robust Pasteur effect, enhancing glycolysis in response to an inhibition of mitochondrial ATP synthesis (Kauppinen and Nicholls, 1986b). The Seahorse respirometer can detect the resultant lactate release as an extracellular acidification. Fig. 2D shows that the rate of acidification in glucose medium increases on addition of oligomycin, consistent with an activation of anaerobic glycolysis as compensation for the inhibited mitochondrial ATP synthesis. Acidification rates in the presence of glucose plus pyruvate were similar, and in both cases the further addition of FCCP resulted in a further increase in rate. In glucose-free pyruvate medium as expected no increase is seen on addition of oligomycin, but FCCP produces an increased acidification. Since the FCCP addition is in each case associated with a large enhancement of respiration this suggests that CO_2 evolution from the TCA cycle can contribute to the medium acidification detected in the medium. The slow decline in acidification rate, as well as in respiration, seen after FCCP in the presence of oligomycin is a consistent feature in these experiments and may be a consequence of the acidification of the the cytoplasm and matrix occurring under these conditions.

Pyruvate metabolism

α-Cyanocinnamate is an inhibitor of the mitochondrial inner membrane pyruvate transporter (Hildyard et al., 2005). The dominant role of pyruvate as a substrate for the *in situ* mitochondria is shown by the extensive concentration dependent inhibition of the spare respiratory capacity (Fig. 4A). It is notable that no significant effect of the inhibitor is seen on basal or oligomycin inhibited respiration, indicating that the respiratory limitation following addition of the transport inhibitor is only apparent under conditions of maximal pyruvate utilization, i.e. pyruvate transport and pyruvate dehydrogenase have little control over the basal respiration rate. Since the activity of pyruvate dehydrogenase is inhibited by pyruvate dehydrogenase kinase it is of interest to establish whether the dehydrogenase is maximally activated under these conditions. Dichloroacetate inhibits the kinase, and hence maximizes pyruvate dehydrogenase activity (Fuller and Randle, 1984). Titration of synaptosomes with up to 1 mM dichloracetate failed to affect basal, oligomycin inhibited or FCCP stimulated respiration, and no effect on lactate extrusion (as monitored by the extra-

cellular acidification rate) was detected (data not shown). This supports earlier indications that pyruvate dehydrogenase has little control over respiration in synaptosomal preparations (Kauppinen and Nicholls 1986a). Mitochondrial oxidation of glycolytic pyruvate is dependent upon the oxidation of cytoplasmic NADH. The importance of the malate/aspartate shuttle in this context (Kauppinen et al., 1987) is demonstrated by the inhibition of spare respiratory capacity in the presence of the transaminase inhibitor aminoxyacetic acid (Fig. 4B).

Mitochondrial coupling to plasma membrane ion fluxes

The presynaptic Na^+/K^+-ATPase is a major utilizer of ATP under conditions when sodium reentry is enhanced, for example following addition of veratridine to prevent inactivation of voltage activated sodium channels (Nicholls and Scott, 1980). The effect of veratridine on the respiration of the cortical synaptosomes in glucose/pyruvate medium is shown in Fig. 5A, B. An extensive enhancement of respiration is seen, accompanied by an increase in extracellular acidification (Fig 5C, D). The stimulation of respiration is oligomycin sensitive (Fig. 5B) consistent with the enhanced ATP turnover, however a slight increase in oligomycin-insensitive respiration is seen, possibly due to an increase in the rate of Ca^{2+} cycling across the inner membrane driven by the proton circuit as a consequence of activation of mitochondrial Na^+/Ca^{2+} exchanger by the increased cytoplasmic Na^+ (Nicholls and Scott 1980).

In glucose plus pyruvate medium the veratridine-stimulated respiration was accompanied by a reciprocal decline in FCCP-stimulated respiration both in the presence or absence of oligomycin (Fig. 5A, B). Veratridine also caused a parallel decrease in the extra-cellular acidification rate (Fig. 5C, D), indicative of a limitation in glycolysis. Consistent with this, veratridine addition in glucose-only medium led to an almost complete loss of FCCP-stimulated respiration (data not shown).

On purely bioenergetic grounds addition of the Na^+/K^+-ATPase inhibitor ouabain would be predicted to cause a decreased respiration by inhibiting the slow ATP hydrolysis by the pump under basal conditions. In practice, however a slight stimulation of respiration is seen on addition of the inhibitor (Fig. 6A) which was sensitive to oligomycin and thus due to increased mitochondrial ATP-turnover. Since ouabain induces plasma membrane depolarization and allows cytoplasmic Na^+ to rise, it is possible that the combination of the ATP requirement for exocytosis and enhanced Na^+ and Ca^{2+} cycling at the mitochondrial inner membrane more than compensates for the decreased ATP requirement by the Na^+/K^+-ATPase. In glucose plus pyruvate medium following oligomycin, the presence of 0.3mM ouabain decreased FCCP-stimulated respiration from 860±146% to 592±38% of the glucose-only basal respiration. More dramatically, ouabain almost completely abolished the spare respiratory capacity in glucose-only medium (data not shown). Thus ouabain, similarly to veratridine, inhibited glycolysis. Therefore another possible explanation is that ouabain increased respiration as compensation for the decreased contribution of glycolysis to ATP turnover.

The bioenergetic demand of repetitive action potential firing

Veratridine is a use-dependent inhibitor of sodium channel deactivation, and its effectiveness in this and other synaptosomal preparations indicates that the terminals undergo slow spontaneous action potential firing in low K^+ medium. The potassium channel inhibitor 4-aminopyridine (4AP) greatly enhances the frequency of these spontaneous action potentials, and has been extensively employed in studies with isolated synaptosomes to induce trains of repetitive action potentials to study the mechanism and regulation of transmitter exocytosis (Tibbs et al., 1989a). 4AP should increase synaptosomal ATP demand

as the terminal restores ionic homeostasis following action-potential initiated calcium and sodium entry, in addition to the ATP requirements of exocytosis and endocytosis. Concentrations of 50μM and 1mM 4AP respectively induce half-maximal and maximal glutamate exocytosis from cortical synaptosomes (Tibbs *et al.* 1989) and these concentrations were employed here, producing a graded respiratory response (Fig. 6B). In contrast to veratridine and ouabain, 4AP did not significantly reduce FCCP stimulated respiration (903±66% control, 819±41% in presence of 1mM 4AP).

Loss of spare respiratory capacity and enhanced susceptibility to stochastic mitochondrial depolarization of synaptosomes with restricted electron transport activity

Brain mitochondria prepared from rodent models of many major neurodegenerative disorders show impaired electron transport activity (reviewed in (Lin and Beal 2006). Since brain mitochondrial preparations are an inherently heterogeneous mixture originating from processes, terminals, cell bodies and glia, it is difficult to make conclusions relating the *in vitro* mitochondrial dysfunction to functional deficits or pathology. As a preliminary to investigating these and additional disease models, synaptosomes were titrated with low concentrations of rotenone or 3-nitropropionic acid to partially inhibit Complexes I and II respectively (Fig. 7). It is notable that spare respiratory capacity is titrated down by the inhibitors with no effect on basal or oligomycin-insensitive respiration. In other words the control that electron transport exerts over respiration is expected to be lowest in the presence of oligomycin, when proton re-entry has greatest control, Conversely, electron transport will have greatest control under conditions of maximal electron flux when proton re-entry is not restricted (Brand, 2005).

The ability to image single synaptosomes allows us to test one aspect of the 'spare respiratory capacity' concept, namely that statistical deviations in individual terminals that result in a bioenergetic deficit can result in stochastic mitochondrial depolarization within the population, and that this is exacerbated by factors that restrict maximal electron transport activity. In order to determine the viability of the synaptosomes in the face of a relatively modest increase in proton current demand, single synaptosomes were tracked and the changes of $TMRM^+$ fluorescence intensity were recorded under control conditions or during application of rotenone or 3NPA at concentrations that partially restricted spare respiratory capacity (10 nM and 200 μM respectively, Fig. 7).

The mean $\Delta\psi_m$ was only slightly decreased compared to the untreated control by rotenone (by 7.1±1.2 mV) or 3NPA (by 6.5±1.8 mV) at 34 min after application of the inhibitors (n=10 synaptosomal preparations; $p<0.05$). It should be noted that the synaptosomes retain considerable spare respiratory capacity in the presence of these inhibitor concentrations (Fig. 7). However, partial electron transport inhibition results in a broadening of the spread in mitochondrial membrane potentials in the individual terminals (Fig. 8 A, C, E) signified by the greater standard deviation of $\Delta\psi_m$ (10.5±0.4 mV for rotenone and 10.5±0.8 mV for 3NPA, compared with 7.4±0.3 mV for the control at t=34 min; $p<0.001$; n=10.

In order to simulate an increase in energy demand, synaptosomes were treated with a very low concentration of FCCP (150 nM in the presence of 64μM BSA), which alone caused only an insignificant decrease in mean $\Delta\psi_m$ (2.7±1.5 mV at t=34 min; $p>0.05$). When 10nM rotenone was combined with this FCCP concentration, $\Delta\psi_m$ gradually decreased (by 13.2±1.8 mV at t=34 min, as compared to the untreated control; $p<0.001$; n=4), while a subset of synaptosomes was depolarized by more than 30 mV, sufficient to abolish mitochondrial ATP production. At 34min, 5.9±0.6% of the rotenone plus FCCP population passed this threshold vs. 1.1±0.2% for the control plus FCCP ($p<0.05$). The progressive nature of the depolarization meant that by 79min 37.9±9.3% vs. 4.5±0.3% respectively of the populations had depolarized by more than 30mV. Qualitatively similar results were

obtained for 3NPA-inhibited synaptosomes (11.7±2.6 mV depolarization at t=34 min, $p<0.01$; n=4) for the combination of 3NPA and FCCP.

Discussion

Methodology

The synaptosome preparation has been available for almost 50 years (reviewed in Whittaker, 1993) and was subsequently refined with techniques to improve purity (Dunkley *et al.* 2008). Included among the more than 10,000 references exploiting the preparation are studies monitoring mitochondrial and plasma membrane potentials and respiration (e.g. Nicholls and Scott, 1980), presynaptic substrate metabolism (Erecinska *et al.* 1996) and oxidative stress (Tretter and Adam-Vizi 2007), glutamate release (e.g. Nicholls and Sihra, 1986) and the molecular mechanisms of vesicular trafficking (Cousin and Robinson 2000). The ability of 4AP to induce spontaneous 'action potentials' (Tibbs et al., 1989a) allowed presynaptic receptor regulation of exocytosis to be studied in great detail (Sánchez-Prieto et al., 1996). However, while synaptosomes can be prepared from animals of any age, the amount of material required to monitor respiration (typically 0.5mg protein) has limited the study of the presynaptic bioenergetics of specific brain regions of transgenic mice unless large numbers of animals are sacrificed. The present technique reduces the amount of material required to monitor respiration by a factor of 50.

Spare respiratory capacity

An important aspect of aging-related changes in the brain is that loss of function is gradual, suggestive of a stochastic synaptic failure. Studies with cultured neurons exposed to energy-intensive excitotoxic stress have supported a hypothesis that neuronal cell death in this context is primarily induced by an 'energy crisis' (Nicholls et al., 2007). Thus reduction of spare respiratory capacity or maximal ATP generation by oxidative damage to *in situ* mitochondria (Vesce et al., 2005), Complex I restriction (Yadava and Nicholls, 2007), 'mild-uncoupling' (in an attempt to reduce oxidative stress, Johnson-Cadwell et al., 2007) or oxygen-glucose deprivation (Vesce and Nicholls, unpublished) each potentiate glutamate-induced cell death concomitant with an exhaustion of spare respiratory capacity in the neuronal cultures. The present combination of population respiration studies of spare respiratory capacity with single synaptosomal fluorescence monitoring of membrane potential allows the stochastic model of presynaptic bioenergetic failure to be tested. In particular we propose that the simple initial experiment quantifying respiration under basal conditions, in the presence of oligomycin and following carefully titrated protonophore be adopted as an initial quantitative means of assessing the rather vague concept of mitochondrial dysfunction. Basal respiration in the presence of substrate drives both proton leak and ATP synthesis. Addition of oligomycin eliminates proton re-entry via the ATP synthase and the decrease in respiration provides a minimum estimate of the proton current used to drive ATP synthesis prior to addition of the inhibitor. However, since the proton leak is voltage-dependent (Nicholls, 1974; Nobes et al., 1990) the mitochondrial hyperpolarization that accompanies ATP-synthase inhibition will enhance the proton leak and hence lead to some under-estimation of the ATP-synthesizing proton current and proportionate over-estimation of the proton leak under normal sub-maximal 'State 3½' ATP-generating conditions (i.e. intermediate between State 3 and State 4).

Damage to, and inhibition of, electron transport chain complexes is central to many neurodegenerative disorders (Beal, 2005). Neuronal mitochondria are subjected to a variable ATP demand, depending primarily on their excitation pattern, and it is critical that the electron transport chain has sufficient capacity to supply protons to the ATP synthase. We have coined the term 'spare respiratory capacity'to quantify the difference between this

maximal uncontrolled respiration and the initial basal respiration (Nicholls et al., 2007) and have proposed that the maintenance of some spare respiratory capacity even under conditions of maximal physiological or pathophysiological stimulus is a major factor defining the survival of the neuron.

Synaptosomal bioenergetics

The present study has allowed us to reproduce and extend earlier findings with rat or guinea-pig cerebrocortical synaptosomes obtained with conventional oxygen electrode respirometry. The ability of exogenous pyruvate to synergize with glucose was shown earlier (Kauppinen and Nicholls, 1986a). In the present study this is shown to be due to a variable hyperpolarization (depending on the glycolytic competence of a given synaptosome) throughout the synaptosomal population. The implication is that glycolysis slowly deteriorates in synaptosomes incubated at 37°C, as shown by the progressive decrease in $\Delta\psi_m$ and that this metabolic limitation can be rescued by inclusion of exogenous pyruvate. Pyruvate does not however prevent the slow decline in maximal respiration following FCCP (see e.g. Fig. 2) suggesting that mitochondrial respiration does not continue indefinitely in a terminal whose sources of ATP (failing glycolysis and uncoupled mitochondria) are severely compromised. In an earlier study (Kauppinen and Nicholls, 1986c)a progressive failure of glycolysis and ATP depletion were reported following cyanide inhibition of respiration.

The inability of dichloracetate to further activate pyruvate dehydrognase in mouse synaptosomes, the role of the malate-aspartate shuttle in reoxidizing cytoplasmic NADH during glycolysis, and the increased respiration consequent upon Na^+ channel activation by veratridine are consistent with earlier studies (Nicholls and Scott, 1980, Kauppinen and Nicholls, 1986a, Kauppinen et al., 1987). While we introduced 4AP as a means of inducing spontaneous action potentials in synaptosomes (Tibbs et al., 1989a,b) the energetic demand of exo-endocytosis and the re-establishment of ionic homeostasis has not previously been documented. It is significant that, relative to 'quiescent' synaptosomes in 3.5mM KCl medium, firing induced by 1mM 4AP at least doubles synaptosomal ATP turnover (Fig. 6).

Both in the presence and absence of oligomycin, veratridine decreases the maximal respiration achievable with FCCP (Fig. 5). Veratridine acts by preventing Na^+ channel desensitization and thus increases Na^+ cycling and ATP utilization by the Na^+ pump, as is reflected in the increased oligomycin-sensitive respiration. At the same time it elevates cytoplasmic Na^+ causing extensive efflux of glutamate and aspartate from the cytoplasm by reversal of the excitatory amino acid carrier (Seal and Amara 1999). In view of the importance of the malate/aspartate shuttle, evidenced from the inhibitory effect of AOAA (Fig. 4B), it is possible that cytoplasmic aspartate depletion may limit the activity of the shuttle and hence glycolysis. However application of exogenous aspartate did not rescue the spare respiratory capacity (data not shown).

Ouabain reduced spare respiratory capacity similarly to veratridine in glucose plus pyruvate medium. In both cases this effect was amplified in glucose-only medium, suggesting an inhibition of glycolysis. Indeed a time-dependent inhibition of glycolysis has been reported in rat brain synaptosomes in the presence of veratridine and ascribed to an inhibition of hexokinase as a result of ATP depletion (Erecinska *et al.* 1996). However, in contrast to veratridine, ouabain preserves synaptosomal ATP (Nicholls and Scott, 1980), therefore it is unlikely that ATP depletion fully accounts for the respiratory decline. A common feature of both veratridine and ouabain is that both trigger a sustained increase of $[Na^+]_i$ paralleled by a further decrease in $[K^+]_I$, i.e. a collapse of the plasma membrane Na^+-electrochemical potential. The isolated nerve terminal is deprived of physiological neurotrophic factors and there are suggestions that this may underlie a time-dependent decline in glucose and

glutamate transport that can be prevented by neurotrophic factors (Guo and Mattson 2000). Finally, synaptosomes have a low internal K^+ concentration as a result of the isolation procedure (Nicholls & Scott 1980). Since K^+ is a necessary co-factor for pyruvate kinase (Kachmar & Boyer 1953) inhibition of this enzyme as a consequence of the loss of cytosolic K^+ is an alternative explanation for the inhibition of the glycolysis.

Loss of spare respiratory capacity and enhanced stochastic mitochondrial depolarization following restricted electron transport activity

There is convincing evidence associating a partial inhibition of Complex I with Parkinson's Disease (reviewed in (Beal 2005). The association of Complex II deficiency with Huntington's is more tenuous (reviewed in (Browne and Beal 2004;Orr *et al.* 2008). In the case of PD, degeneration of the nigro-striatal dopaminergic neurons may occur in a retrograde manner (Betarbet *et al.* 2006), emphasizing the relevance of investigating presynaptic striatal bioenergetics. There is a major conceptual problem in relating acute experiments to the slow progression of the human neurodegenerative disorders. We have proposed that the failure of a synapse may occur stochastically when that terminal faces an 'energy crisis', i.e. when the instantaneous ATP demand in that terminal exceeds the maximal ATP supply by the combination of oxidative phosphorylation and glycolysis (Nicholls *et al.* 2007). Such an event may be rare, a bioenergetic 'hundred year flood' but as mitochondrial capacity declines with age (Lenaz *et al.* 2006) the probability of stochastic failure will increase, contributing to the age-related component in the incidence of the neurodegenerative disorders. Spare respiratory capacity is thus a critical factor in maintaining a reserve of ATP generating capacity.

Preparations of isolated brain mitochondria are inherently heterogeneous reflecting the multiple cell types and sub-cellular localizations. In particular the expression of cyclophilin D and the associated susceptibility to the permeability transition is variable. At the single mitochondrion level isolated brain mitochondria undergo stochastic oscillations in $\Delta\psi$ that appear to be associated with the permeability transition since they are decreased by exogenous ADP (Vergun et al., 2003,Vergun and Reynolds 2004). Hazelton et al. (2008) have reported that cyclophilin D is preferentially expressed in GABAergic interneurons, with lower expression in synaptic rather than non-synaptic mitochondria, contrasting with an opposite conclusion on sub-cellular sensitivity from Naga et al. (2007). Conversely, mitochondria prepared from glutamatergic cerebellar granule neurons were insensitive to cyclosporine A in contrast to cortical astrocytes (Bambrick *et al.* 2006). Nayak et al. (1999) have reported a heterogeneous distribution of serotonin receptors on individual synaptosomes from different brain regions. Finally, sensitivity to excitotoxicity differs widely in different neuronal cultures and although much of this can be ascribed to differential NMDA receptor expression, the role of mitochondria remains unclear.

Conclusions

We have described sensitive techniques for monitoring and quantifying bioenergetic function in isolated nerve terminals acutely from a specific mouse brain region. Since synaptosomes may be prepared from animals of any age and are used acutely, they represent an *ex vivo* preparation that can faithfully represent the metabolism of the intact terminal in the animal before sacrifice. The approach is thus invaluable for investigating aging-related aspects of presynaptic function in a wide variety of transgenic and disease models.

Acknowledgments

This work was supported by grants from the NIH (P01 AG025901) and the Keck Foundation 'Why aging causes disease'.

Abbreviations

3NPA	3-nitropropionic acid
4AP	4-aminopyridine
CCIN	α-cyanocinnamate
$\Delta\psi_m$	mitochondrial membrane potential
FCCP	carbonylcyanide-*p*-trifluoromethoxy-phenylhydrazone
TMRM	tetramethylrhodamine methyl ester

References

Bambrick LL, Chandrasekaran K, Mehrabian Z, Wright C, Krueger BK, Fiskum G. Cyclosporin A increases mitochondrial calcium uptake capacity in cortical astrocytes but not cerebellar granule neurons. J Bioenerg. Biomembr. 2006; 38:43–47. [PubMed: 16786428]

Beal MF. Mitochondria take center stage in aging and neurodegeneration. Ann. Neurol. 2005; 58:495–505. [PubMed: 16178023]

Betarbet R, Canet-Aviles RM, Sherer TB, Mastroberardino PG, McLendon C, Kim JH, Lund S, Na HM, Taylor G, Bence NF, Kopito R, Seo BB, Yagi T, Yagi A, Klinefelter G, Cookson MR, Greenamyre JT. Intersecting pathways to neurodegeneration in Parkinson's disease: effects of the pesticide rotenone on DJ-1, alpha-synuclein, and the ubiquitin-proteasome system. Neurobiol. Dis. 2006; 22:404–420. [PubMed: 16439141]

Brand MD. The efficiency and plasticity of mitochondrial energy transduction. Biochem. Soc. Trans. 2005; 33:897–904. [PubMed: 16246006]

Browne SE, Beal MF. The energetics of Huntington's disease. Neurochem. Res. 2004; 29:531–546. [PubMed: 15038601]

Cousin MA, Robinson PJ. Two mechanisms of synaptic vesicle recycling in rat brain nerve terminals. J. Neurochem. 2000; 75:1645–1653. [PubMed: 10987846]

Dunkley PR, Jarvie PE, Heath JW, Kidd GJE, Rostas JAP. A rapid method for isolation of synaptosomes on percoll gradients. Brain Re.s. 1986; 372:115–129.

Dunkley PR, Jarvie PE, Robinson PJ. A rapid Percoll gradient procedure for preparation of synaptosomes. Nat. Protoc. 2008; 3:1718–1728. [PubMed: 18927557]

Erecinska M, Nelson D, Deas J, Silver IA. Limitation of glycolysis by hexokinase in rat brain synaptosomes during intense ion pumping. Brain Res. 1996; 726:153–159. [PubMed: 8836555]

Fuller SJ, Randle PJ. Reversible phosphorylation of pyruvate dehydrogenase in rat skeletal-muscle mitochondria. Effects of starvation and diabetes. Biochem. J. 1984; 219:635–646. [PubMed: 6331393]

Gerencser AA, Nicholls DG. Measurement of instantenous velocity vectors of organelle transport: application to mitochondrial transport in hippocampal neurons. Biophys. J. 2008; 95:3079–3099. [PubMed: 18757564]

Guo ZH, Mattson MP. Neurotrophic factors protect cortical synaptic terminals against amyloid and oxidative stress-induced impairment of glucose transport, glutamate transport and mitochondrial function. Cereb. Cortex. 2000; 10:50–57. [PubMed: 10639395]

Hazelton JL, Petrasheuskaya M, Fiskum G, Kristian T. Cyclophilin D is expressed predominantly in mitochondria of gamma-aminobutyric acidergic interneurons. J Neurosci. Res. 2008; 87:1250–1259. [PubMed: 18951528]

Hildyard JC, Ammala C, Dukes ID, Thomson SA, Halestrap AP. Identification and characterisation of a new class of highly specific and potent inhibitors of the mitochondrial pyruvate carrier. Biochim Biophys Acta. 2005; 1707:221–230. [PubMed: 15863100]

Johnson-Cadwell LI, Jekabsons MB, Wang A, Polster BM, Nicholls DG. 'Mild uncoupling' does not decrease mitochondrial superoxide levels in cultured cerebellar granule neurons but decreases

spare respiratory capacity and increases toxicity to glutamate and oxidative stress. J Neurochem. 2007; 101:1619–1631. [PubMed: 17437552]

Jones DG, Brearley RF. An analysis of some aspects of synaptosomal ultrastructure by the use of serial sections. Cell and Tissue Res. 1973; 140:481–496.

Kachmar J, Boyer PD. Kinetic analysis of enzyme reactions. II. The potassium activation and calcium inhibition of pyruvic phosphoferase. J. Biol Chem. 1953; 200:669–682. [PubMed: 13034826]

Kauppinen RA, Nicholls DG. Pyruvate utilization by synaptosomes is independent of calcium. FEBS Lett. 1986a; 199:222–226. [PubMed: 3084295]

Kauppinen RA, Nicholls DG. Synaptosomal bioenergetics: The role of glycolysis, pyruvate oxidation and responses to hypoglycaemia. Eur. J. Biochem. 1986b; 158:159–165. [PubMed: 2874024]

Kauppinen RA, Nicholls DG. Failure to maintain glycolysis in anoxic nerve terminals. J. Nurochem. 1986c; 47:1864–1869.

Kauppinen RA, Sihra TS, Nicholls DG. Aminoxyacetic acid inhibits the malate-aspartate shuttle in isolated nerve terminals and prevents the mitochondria from utilizing glycolytic substrates. Biochim Biophys Acta. 1987; 930:173–178. [PubMed: 3620514]

Lenaz G, Baracca A, Fato R, Genova ML, Solaini G. New insights into structure and function of mitochondria and their role in aging and disease. Antioxid. Redox. Signal. 2006; 8:417–437. [PubMed: 16677088]

Lin MT, Beal MF. Mitochondrial dysfunction and oxidative stress in neurodegenerative diseases. Nature. 2006; 443:787–795. [PubMed: 17051205]

Millán C, Luján R, Shigemoto R, Sánchez-Prieto J. Subtype-specific expression of group III metabotropic glutamate receptors and Ca^{2+} channels in single nerve terminals. J. Biol. Chem. 2002; 277:47796–47803. [PubMed: 12376542]

Naga KK, Sullivan PG, Geddes JW. High cyclophilin D content of synaptic mitochondria results in increased vulnerability to permeability transition. J. Neurosci. 2007; 27:7469–7475. [PubMed: 17626207]

Nayak SV, Dougherty JJ, McIntosh JM, Nichols RA. Ca^{2+} changes induced by different presynaptic nicotinic receptors in separate populations of individual striatal nerve terminals. J. Neurochem. 2001; 76:1860–1870. [PubMed: 11259504]

Nicholls DG. The influence of respiration and ATP hydrolysis on the proton electrochemical potential gradient across the inner membrane of rat liver mitochondria as determined by ion distribution. Eur. J. Biochem. 1974; 50:305–315. [PubMed: 4452361]

Nicholls DG. The glutamatergic nerve terminal. Eur. J. Biochem. 1993; 212:613–631. [PubMed: 8096460]

Nicholls DG. Bioenergetics and Transmitter Release in the Isolated Nerve Terminal. Neurochem. Res. 2003; 28:1431–1439.

Nicholls DG, Johnson-Cadwell LI, Vesce S, Jekabsons MB, Yadava N. The bioenergetics of mitochondria in cultured neurons and their role in glutamate excitotoxicity. J. Neurosci. Res. 2007; 85:3206–3212. [PubMed: 17455297]

Nicholls DG, Scott ID. The regulation of brain mitochondrial calcium-ion transport: the role of ATP in the discrimination between kinetic and membrane-potential-dependent Ca efflux mechanisms. Biochem. J. 1980; 186:833–839. [PubMed: 7396840]

Nicholls DG, Sihra TS. Synaptosomes possess an exocytotic pool of glutamate. Nature. 1986; 321:772–773. [PubMed: 3713864]

Nichols RA, Mollard P. Direct observation of serotonin 5-HT_3 receptor-induced increases in calcium levels in individual brain nerve terminals. J. Neurochem. 1996; 67:581–592. [PubMed: 8764583]

Nobes CD, Brown GC, Olive PN, Brand MD. Non-ohmic proton conductance of the mitochondrial inner membrane in hepatocytes. J. Biol. Chem. 1990; 265:12903–12909. [PubMed: 2376579]

Orr AL, Li S, Wang CE, Li H, Wang J, Rong J, Xu X, Mastroberardino PG, Greenamyre JT, Li XJ. N-terminal mutant huntingtin associates with mitochondria and impairs mitochondrial trafficking. J. Neurosci. 2008; 28:2783–2792. [PubMed: 18337408]

Otsu N. A threshold selection method from gray-level histograms. IEEE Trans. Syst. Man Cybern. 1979; 9:66–66.

Sánchez-Prieto J, Budd DC, Herrero I, Vázquez E, Nicholls DG. Presynaptic receptors and the control of glutamate exocytosis. Trends Neurosci. 1996; 19:235–239. [PubMed: 8761959]

Seal RP, Amara SG. Excitatory amino acid transporters: A family in flux. Annu. Rev. Pharmacol. Toxicol. 1999; 39:431–456. [PubMed: 10331091]

Scott ID, Nicholls DG. Energy transduction in intact synaptosomes: influence of plasma- membrane depolarization on the respiration and membrane potential of internal mitochondria determined in situ. Biochem. J. 1980; 186:21–33. [PubMed: 7370008]

Stigliani S, Zappettini S, Raiteri L, Passalacqua M, Melloni E, Venturi C, Tacchetti C, Diaspro A, Usai C, Bonanno G. Glia re-sealed particles freshly prepared from adult rat brain are competent for exocytotic release of glutamate. J. Neurochem. 2006; 96:656–668. [PubMed: 16405496]

Tibbs GR, Barrie AP, Van-Mieghem F, McMahon HT, Nicholls DG. Repetitive action potentials in isolated nerve terminals in the presence of 4-aminopyridine: effects on cytosolic free Ca^{2+} and glutamate release. J. Neurochem. 1989a; 53:1693–1699. [PubMed: 2553862]

Tibbs GR, Dolly JO, Nicholls DG. Dendrotoxin, 4-aminopyridine, and beta-bungarotoxin act at common loci but by two distinct mechanisms to induce Ca^{2+}- dependent release of glutamate from guinea-pig cerebrocortical synaptosomes. J. Neurochem. 1989b; 52:201–206. [PubMed: 2562805]

Tretter L, Adam-Vizi V. Uncoupling is without an effect on the production of reactive oxygen species by in situ synaptic mitochondria. J. Neurochem. 2007; 103:1871.

Vergun O, Reynolds IJ. Fluctuations in mitochondrial membrane potential in single isolated brain mitochondria: Modulation by adenine nucleotides and Ca^{2+} Biophys. J. 2004; 87:3585–3593. [PubMed: 15315954]

Vergun O, Votyakova TV, Reynolds IJ. Spontaneous changes in mitochondrial membrane potential in single isolated brain mitochondria. Biophys. J. 2003; 85:3358–3366. [PubMed: 14581237]

Vesce S, Jekabsons MB, Johnson-Cadwell LI, Nicholls DG. Acute glutathione depletion restricts mitochondrial ATP export in cerebellar granule neurons. J. Biol. Chem. 2005; 280:38720–38728. [PubMed: 16172117]

Ward MW, Rego AC, Frenguelli BG, Nicholls DG. Mitochondrial membrane potential and glutamate excitotoxicity in cultured cerebellar granule cells. J. Neurosci. 2000; 20:7208–7219. [PubMed: 11007877]

Whittaker VP. Thirty years of synaptosome research. J. Neurocytol. 1993; 22:735–742. [PubMed: 7903689]

Wu M, Neilson A, Swift AL, Moran R, Tamagnine J, Parslow D, Armistead S, Lemire K, Orrell J, Teich J, Chomicz S, Ferrick DA. Multiparameter metabolic analysis reveals a close link between attenuated mitochondrial bioenergetic function and enhanced glycolysis dependency in human tumor cells. Am. J Physiol Cell Physiol. 2007; 292:C125–C136. [PubMed: 16971499]

Yadava N, Nicholls DG. Spare respiratory capacity rather than oxidative stress regulates glutamate excitotoxicity following partial respiratory inhibition of mitochondrial complex I with rotenone. J. Neurosci. 2007; 27:7310–7317. [PubMed: 17611283]

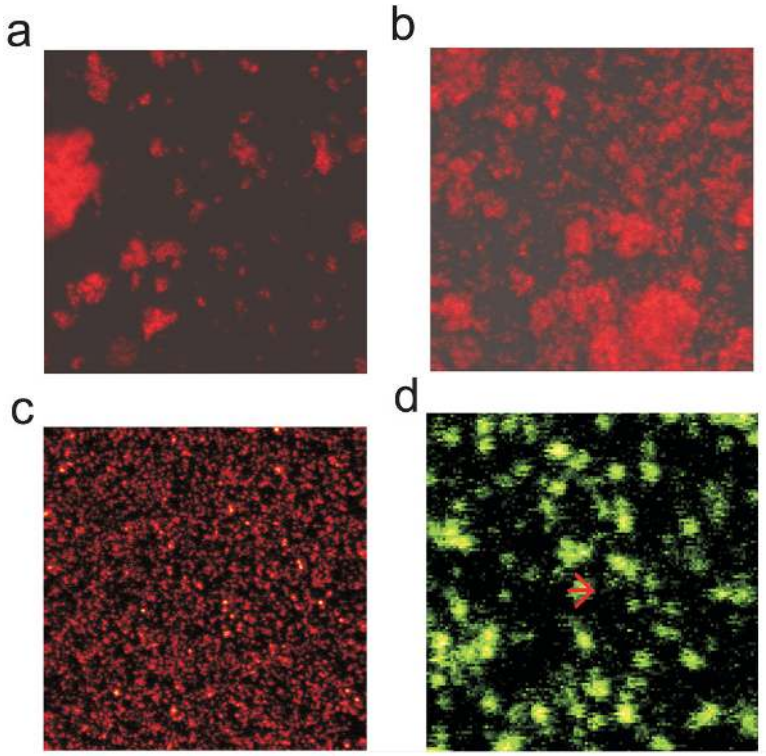

Fig. 1.

Confocal imaging of synaptosomes equilibrated with 50nM TMRM. Synaptosomes in 'Ionic Medium' were allowed to sediment under unit gravity (a) or by centrifugation at 3400g (b) for 60 min prior to imaging. (c) Synaptosomes in sucrose medium were centrifuged in parallel. The field size was 115 × 115μm. (d) Enlarged area from 'c'. The density profile across a representative particle (arrow) gives a diameter of 1.8μm, typical for a synaptosome.

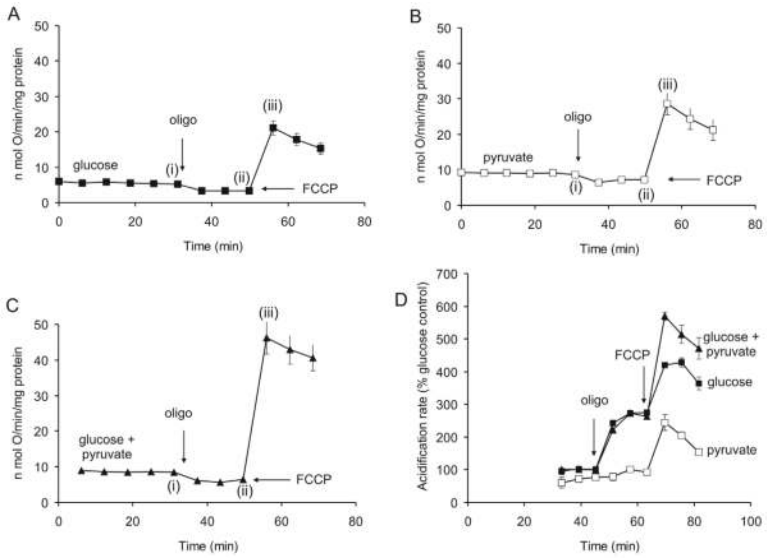

Fig. 2.

Basic respiratory parameters for cortical synaptosomes: ATP synthase inhibition and FCCP release of respiratory control. Substrates initially present were (A), 15mM glucose, (B) 10mM pyruvate or (C) 15mM glucose + 10mM pyruvate. Further additions were 4μg/ml oligomycin (oligo) and 4μM FCCP. Rates at the time-points (i) to (iii) are given in Table 1. (D) Rates of extra-cellular acidification determined in parallel with respiration; results are normalized to the acidification rate in glucose medium prior to addition of oligomycin.

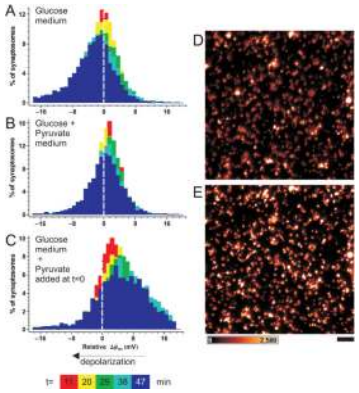

Fig. 3.

Time-dependent changes in $\Delta\psi_m$ in individual synaptosomes: pyruvate causes a general, rather than selective, mitochondrial hyperpolarization. 'Sucrose' synaptosomes were equilibrated with 10nM $TMRM^+$. (A-C) Colours represent histograms of the change in $\Delta\psi_m$ in individual synaptosomes, relative to t=0, sampled at the indicated times. Negative millivolts indicate relative depolarization. Synaptosomes in A and B were equilibrated with glucose and glucose+ pyruvate media respectively, while in C 10mM pyruvate was added to synaptosomes in glucose-only medium after the t=0 time-point. (D-E) false colour intensity image of before (D) and 38min after (E) addition of pyruvate to a field of synaptosomes in glucose-only medium. Scale bar 5μm, intensity scale is shown in arbitrary units of a 12-bit digitizer.

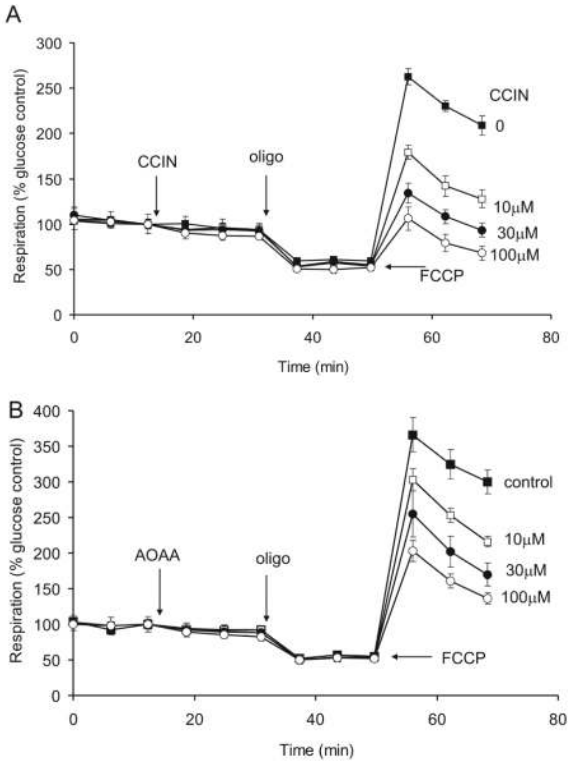

Fig. 4.

α-Cyanocinnamate and aminoxyacetate inhibition of FCCP-stimulated respiration. (A) 15mM glucose was present initially as substrate. Where indicated, 0-100μM α-cyanocinnamate (CCIN) was added followed by 4μg/ml oligomycin (oligo) and 4μM FCCP. (B) 0-100μM aminoxyacetate (AOAA) was added where indicated. In these and subsequent experiments respiration is calculated relative to basal respiration in glucose medium.

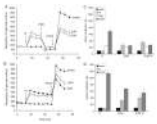

Fig. 5.

Veratridine enhancement of mitochondrial ATP turnover and inhibition of FCCP-stimulated respiration (A) in the presence and (B) in the absence of oligomycin. Synaptosomes were incubated in the presence of 15mM glucose + 10mM pyruvate. Where indicated veratridine (Vt, 0-5μM), oligomycin (oligo, 4μg/ml) and FCCP (4μM) were added. Rates are expressed relative to basal respiration in medium containing glucose but no pyruvate. (C, D) Corresponding relative acidification rates in the medium.

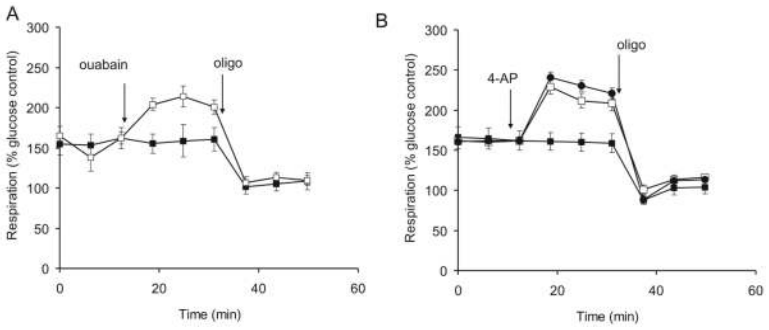

Fig. 6.

Ouabain and 4-aminopyridine enhance oligomycin-sensitive respiration. Synaptosomes were incubated in the presence of 15mM glucose + 10mM pyruvate. (A) Ouabain (0.3mM, open symbols) was added where indicated, followed by oligomycin (4μg/ml). (B) 4-aminopyridine (50μM, open squares or 1mM, circles) was added where indicated, followed by oligomycin (4μg/ml). Rates are expressed relative to basal respiration in medium containing glucose but no pyruvate.

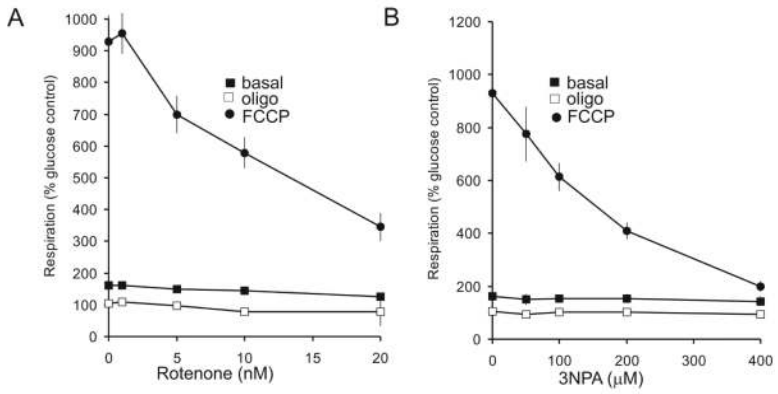

Fig. 7.

Titration of basal, oligomycin-insensitive and FCCP-stimulated respiration with (A) rotenone and (B) 3-NPA. Synaptosomes were incubated in the presence of 15mM glucose + 10mM pyruvate and the indicated concentrations of inhibitors were added during the experiment. Rates are expressed relative to basal respiration in medium containing glucose but no pyruvate.

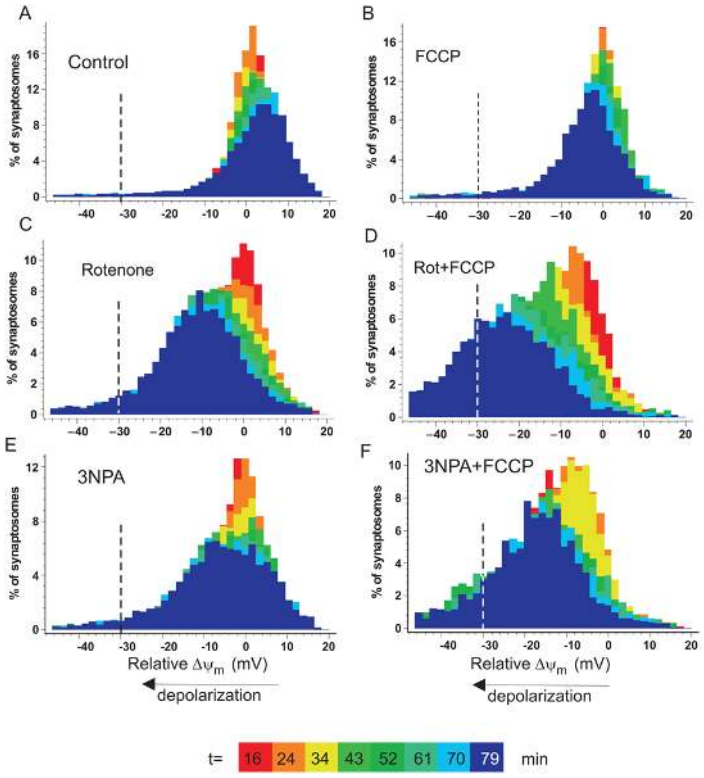

Fig. 8.

Decreased spare respiratory capacity by partial inhibition of Complex I or Complex II accelerates stochastic mitochondrial depolarization. Distribution of $\Delta\psi_m$ in individual synaptosomes. (A) control; (B) plus 150nM FCCP; (C) plus 10nM rotenone, (D) 10nM rotenone plus 150nM FCCP, (E) 200μM 3NPA (F) 200μM 3NPA plus 150nM FCCP. Colors code different time points after inhibitor addition, as indicated. Negative millivolts indicate the relative depolarization compared to the mean of the untreated control at the same time point. The line at −30mV depolarization represents the arbitrary threshold below which the mitochondria would be thermodynamically incapable of ATP generation.

Table 1

Respiration rates of synaptosomes incubated in the presence of 15mM glucose, 10mM pyruvate and glucose plus pyruvate. Data from Fig. 2 taken at the time-points (i) – (iii).

	Respiration (nmol O.min^{-1}.mg protein^{-1})		
Substrates	Basal (i)	+ oligomycin (ii)	+FCCP (iii)
Glucose	5.23±0.72	3.28±0.62	21.11±2.00
Pyruvate	8.60±0.78	6.43±0.84	28.59±3.07
Glucose + Pyruvate	8.47±0.62	6.19±0.52	46.28±4.51